Cigarette smoke induces *miR-132* in Th17 cells that enhance osteoclastogenesis in inflammatory arthritis

Paula B Donate[a], Kalil Alves de Lima[a], Raphael S Peres[a], Fausto Almeida[b], Sandra Y Fukada[c], Tarcilia A Silva[d], Daniele C Nascimento[a], Nerry T Cecilio[a], Jhimmy Talbot[a], Rene D Oliveira[e], Geraldo A Passos[f], José Carlos Alves-Filho[a], Thiago M Cunha[a], Paulo Louzada-Junior[e], Foo Y Liew[g*], Fernando Q Cunha[a].

[a]Department of Pharmacology, Ribeirão Preto Medical School, University of São Paulo, Ribeirão Preto, SP, CEP 14049-900, Brazil.

[b]Departament of Biochemistry and Immunology, Ribeirão Preto Medical School, University of São Paulo, Ribeirão Preto, SP, CEP 14049-900, Brazil.

[c]Department of BioMolecular Sciences, School of Pharmaceutical Sciences, University of São Paulo, São Paulo, SP, CEP 14040-903, Brazil.

[d]Department of Oral Surgery and Pathology, School of Dentistry, Universidade Federal de Minas Gerais, Belo Horizonte, MG, CEP 31270-901, Brazil.

[e]Department of Internal Medicine, Ribeirão Preto Medical School, University of São Paulo, Ribeirão Preto, SP, CEP 14049-900, Brazil.

[f]Molecular Immunogenetics Group, Department of Genetics, Ribeirão Preto Medical School, University of São Paulo, Ribeirão Preto, SP, CEP 14049-900, Brazil.

[g]Division of Immunology, Infection and Inflammation, Glasgow Biomedical Research Centre, University of Glasgow, Glasgow G12 8TA, UK.

*__Corresponding author__ Foo Y Liew: foo.liew@glasgow.ac.uk or Fernando Q Cunha: fdqcunha@fmrp.usp.br

Classification: *Biological Sciences, Immunology and Inflammation*

Key words: Cigarette smoke, Rheumatoid arthritis, Th17, Exosomes, osteoclastogenesis

Author Contributions

P.B.D. planned, performed and analyzed experiments and wrote the manuscript. F.Q.C. and F.Y.L. planned experiments, analyzed data, wrote the manuscript and supervised the project. S.Y.F. and T.A.S. planned and analyzed osteoclasts experiments. F.A. and T.N.C. performed and analyzed EVs experiments. K.A.L., R.S.P., D.C.N. and J.T. performed and analyzed murine experiments. G.A.P. provided reagents and analyzed array experiments. J.C.A.F. and T.M.C. planned and analyzed experiments. R.S.P., R.D.O., S.L.A. and P.LJ. planned, performed and analyzed human experiments.

Abstract

Rheumatoid Arthritis (RA) is a chronic inflammatory disease characterized by joint destruction and severe morbidity. Cigarette smoking (CS) can exacerbate the incidence and severity of RA. Although Th17 cells and the Aryl hydrocarbon Receptor (AhR) have been implicated but the mechanism by which CS induces RA development remains unclear. Here, using transcriptomic analysis we show that *microRNA-132* is specifically induced in Th17 cells under the presence of either AhR agonist or CS-enriched medium. *miRNA-132* thus induced is packaged into extracellular vesicles (EVs) produced by Th17 and acts as a pro-inflammatory mediator increasing osteoclastogenesis through the down regulation of COX-2. *In vivo,* articular knockdown of *miR-132* in murine arthritis models reduces the number of osteoclasts in the joints. Clinically, RA patients express higher levels of *miR-132* than healthy individuals. This increase is further elevated by cigarette smoking. Together, these results reveal a hitherto unrecognized mechanism by which CS could exacerbate RA and further advance understand of the impact of environmental factors on the pathogenesis of chronic inflammatory diseases.

Significance statement

This report reveals a mechanism by which cigarette smoke (CS) could exacerbate local inflammatory disease. CS is a key environmental pollutant affecting millions of people globally and continues to be of considerable interest to the biomedical communities. We found that CS activates the AhR on Th17 cells leading to the up-regulation of *miR-132*, which is then packaged into extracelullar vesicles (EVs) that induce osteoclastogenesis via the suppression of Cox2 that catalyzes prostaglandins. Clinically, rheumatoid arthritis (RA) patients who smoke express higher level of *miRNA-132* compared to non-smoker RA patients. This finding not only reveals a mechanism of CS signalling but may provide a potential target for therapeutic intervention for inflammatory disease in general and RA in particular.

Introduction

RA is a chronic autoimmune disorder that affects about 1% of adult population and is characterized by synovial inflammation and bone destruction, eventually leading to disability (1, 2). The interaction of several genes with environmental and stochastic factors control the onset and development of the disease (3).

Cigarette smoke (CS), a key environmental factor, is highly associated with RA risk and mediates an increase of pro-inflammatory cytokines levels, affecting disease activity (4, 5). CS contains agonists for AhR (6-8). We have previously demonstrated a critical role of AhR on Th17 cells in arthritis development, which is exacerbated by CS (9). While wild-type mice developed exacerbated inflammatory arthritis and elevated frequency of $CD4^{+}IL\text{-}17^{+}$ T cells in the DLN when exposed to CS, $Ahr^{-/-}$ mice did not. Furthermore, an AhR antagonist (CH223191) also blocked the effect of CS in the WT mice (9). However, the molecular mechanism involved in this process is not fully understood. AhR belongs to the helix-loop-helix Per-Arnt-Sim (bHLH-PAS) domain transcription factor family, well known for its response to various external stimuli and regulation of immune system (10-12). In experimental models of arthritis and clinical RA, AhR activation induces pro-inflammatory cytokines production by different cell types, including Th17, fibroblasts and synoviocytes (13, 14). AhR is also

important for maintaining Th17 cells polarization (11, 15-17) characterized by the induction of *RORγt, CYP1A1* and the production of interleukin-17 (18), which plays an important role in RA pathogenesis (19, 20).

CS is also significantly associated with epigenetic modification. MicroRNAs (miRNAs), a class of small non-coding single-stranded RNA with post-transcriptionally regulatory properties (21, 22), play important roles in pathological conditions including RA (23-25). However, the relationship between AhR activation via CS, microRNA and RA pathogenesis is unknown.

In this report, we demonstrate that the transcription of *miR-132*, activated by CS-induced AhR activation in Th17 cells, enhances osteocastogenesis and contributes to the development and progression in experimental RA and clinical RA. The *miR-132* is packaged in extracellular vesicles (EVs) and mediates osteoclastogenesis by the down regulation of *Ptsg2* expression and Cox2 transcription. These results therefore provide a hitherto unrecognized mechanism by which CS could exacerbate local inflammation and joint destruction in RA. Understanding this linkage may provide a key mechanism by which CS exacerbates inflammation in general.

Results

AhR activation induces expression of a specific microRNAs set in Th17 cells.

We first investigated whether AhR activation could affect miRNAs expression in Th17 cells. Naïve T cells ($CD4^+CD44^-CD62L^+$) were purified from the lymph nodes of C57BL/6 mice and polarized to Th17 cells *in vitro* in the presence of IL-6, TGF-β and IL-1. After 72 h, IL-17-producing cells were purified and re-stimulated for 24 h with IL-6, TGF-β, IL-1 and IL-23 in the presence or absence of FICZ (6-formylindolo[3,2-b]carbazole, a well-documented AhR agonist). Th0 condition was used as a control and isolated $CD4^+$ T cells were re-stimulated with IL-2 in the presence or absence of FICZ. Supervised hierarchical clustering analysis identified 224 differentially expressed miRNAs (fold-change $\geq$ 2.0 and FDR $<$ 5%). Among them, 22 miRNAs were up regulated in Th17 cells in the presence of FICZ (Fig. 1*A* and Table S1).

We then matched miRNAs homology between humans and mice, and selected two of the most expressed miRNAs after AhR activation, *miR-132* and *miR-346* (Fig. 1*B*), for validation by quantitative PCR (qPCR). We selected these two miRNAs based on their high level of expression and potential clinical relevance. FICZ markedly increased the expression of these two miRNAs in Th17 cells (Fig. 1*C*). AhR activation by FICZ also increased the expression of *Cyp1a* (the AhR down stream reporter gene) (Fig. 1*D*), IL-17A (Fig. 1*E*), and IL-22 production (Fig. 1*F*). These results demonstrate that AhR activation on Th17 cells induces the expression of *miRNA-132* and *miR-346*, which are highly homologous in mice and humans.

AhR-induced *miR-132* and *miR-346* are correlated with Arthritis development.

Next, we explored if AhR-induced *miR-132* and *miR-346* expression would be associated with the development of inflammatory arthritis using the well-defined murine arthritic models, antigen-induced arthritis (AIA) and collagen-induced arthritis (CIA). In the AIA model, Wild-type (WT) and *Ahr*$^{-/-}$ C57BL/6 mice were primed and boosted with mBSA and injected intraperitoneally with FICZ or vehicle alone. As demonstrated earlier (9), inflammatory arthritis was markedly exacerbated by the treatment with FICZ in the WT mice, whereas *Ahr*$^{-/-}$ mice showed minimal level of disease, which was not affected by the treatment of FICZ. While the expression of *miR-132* and *miR-346* in the Th17 cells from the lymph nodes of the WT mice were significantly enhanced by the treatment of FICZ, the low level of expression of these miRNAs in the Th17 cells of the *Ahr*$^{-/-}$ mice were not affected by the treatment of FICZ (Fig. 2*A*). In the CIA model, DBA/1J mice were primed and boosted with type II collagen and treated intraperitoneally with FICZ or vehicle. As FICZ exacerbated the inflammatory arthritis (9), the treatment also significantly increased the expression of *miR-132* and *miR-346* in the Th17 cells from the lymph nodes of the CIA mice (Fig. 2*B*).

CS contains a variety of AhR agonists (7, 8). We therefore explored the effect of CS on miRNA expression in both AIA and CIA mice exposed to CS during the development of arthritis. As expected, CS exposure significantly exacerbated the inflammatory arthritis (*SI Appendix* Fig. S1). CS markedly increased the expression of *miR-132* and *miR-346* in the Th17 cells from the lymph

nodes of AIA mice (Fig. 2*C*). Supporting this observation, CS also enhanced the expression of *Cyp1a1* (Fig. 2*C*). Similarly, CS enhanced the expression of these 2 miRNAs in the Th17 cells from the lymph nodes of the CIA mice (Fig. 2*D*). Together these results demonstrate that AhR activation leads to increased expression of *miR-132* and *miR-346* in the Th17 cells during inflammatory arthritis.

Increased expression of miRNAs in clinical RA

We next investigated the relevance of the specific expression of *miR-132* and *miR-346* in RA patients. We recruited 37 untreated RA patients and 34 matched healthy individuals (Table S2). $CD4^+$ T cells from the peripheral blood of the RA patients expressed significantly higher levels of human *miR-132* and *miR-346* compared to that of the cells from the healthy controls (Fig. 2*E*). We then stratified the RA patients to non-smokers (n=18) and smokers (n=19). $CD4^+$ T cells from the smoker RA patients expressed significantly higher level of *miR-132* than that of the cells from the non-smokers (Fig. 2*F*). This was accompanied by the higher level of expression of *CYP1A1* in the T cells from the smokers compared to that of the non-smokers. Strikingly, there was no significant difference in the expression of *miR-346* between the T cells from the smoker and non-smoker RA patients (Fig. 2*F*). These results indicate that the data obtained from the experimental murine models of inflammatory arthritis may be applicable to clinical RA. Since the differential expression of *miR-346* was not obvious in the T cells between the smoker and non-smoker RA patients, we focused our investigation on the functional role of *miR-132*.

AhR-induced *miR-132* is released in EVs by Th17 cells

We then investigated the effect of the AhR-induced increase in *miR-132* expression on the function of Th17 cells. Murine naïve T cells ($CD4^+CD44^-CD62L^+$) were purified from the lymph node of WT C57BL/6 mice and polarized to Th17 cells with or without FICZ. The cells were also transfected with anti-miR-132 or scrambled anti-miR. *miR-132* expression was significantly blocked by anti-miR-132, demonstrating the efficacy of the transfection (*SI Appendix* Fig. S2*A*)**.** However, blocking of *miR-132* had no effect on the differentiation of Th17 cells as shown by the percent of $CD4^+$ cell positive for IL-

17A, IFNγ or IL-17A/IL-22 (Fig. S2*B*). *miR-132* also had no effect on established Th17 cells, as transfection of polarized Th17 with anti-miR-132 had no influence on the percent of $CD4^+$ cells expressing IL-17A, IL-17A/IL-22 in the polarized Th17 cells (*SI Appendix* Fig. S2*C*).

We then explored the possible effects of *miR-132* on other Th17 cell functions. Extracellular vesicles (EVs) are an important mechanism of intercellular communication (26). EVs can carry and selectively deliver bioactive molecules such as miRNAs and modulate the activities of receptor cells (27). We therefore explored the possibility that the AhR-induced *miR-132* could be packaged and released to exert its functions on target cells.

Using a series of ultracentrifugation steps, we first purified, characterized and extracted RNA of EV pellets from the supernatants of naïve T cells cultured under the Th17 condition. Nano-tracking analysis revealed an average-size distribution of 123 nm, indicating that Th17 cells are releasing exosomes. We then investigated the potential role of EVs in the function of AhR-activated Th17 in the context of inflammatory arthritis. Naïve $CD4^+$ T cells were sorted from the lymph nodes of C57BL/6 mice and polarized to Th17 in the presence of FICZ. In some cultures, we also added cigarette smoke-enriched medium (CSEM). CSEM has been shown earlier to be a surrogate for CS in *in vitro* culture (9). CSEM was able to enhance Th17 differentiation and increased the expression of *miR-132* (*SI Appendix* Fig. S3). Activation of AhR either by FICZ or CSEM did not significantly affect EVs formation during the Th17 differentiation *in vitro* (*SI Appendix* Fig. S4*A*). Th17-derived EV zeta potential ranged from an average of -8.05 for control cultures to -9.38 after AhR activation. These values suggest that just the contents of the vesicles could be altered by the receptor activation. Western blot analysis shows that the EVs markers tetraspanin CD63 and Argo2 (involved in microRNA biogenesis) were detected in the EVs preparations derived from the Th17 cells (*SI Appendix* Fig. S4*B*).

We next investigated if AhR activation of Th17 cells could affect the expression of *miR-132* in the EV secreted by the Th17 cells. Murine $CD4^+$ T cells were polarized under Th17 condition in the presence of FICZ, CSEM or GW4869 (an inhibitor of EV). Equal number of EVs was collected from the culture supernatant from each treatment and the level of *miR-132* expression determined by

qPCR. FICZ and CSEM significantly increased the expression of *miR-132* in the EVs (Fig. 3*A*). The expression of *miR-132* was completely abolished in the presence of GW4869.

To determine the clinical relevance of this observation, we collected the synovial fluid from 11 smokers and 11 non-smokers RA patients. EVs were harvested from the fluids and analyzed for the expression of *miR-132* by qPCR. The EVs from the smoker RA patients expressed significantly higher levels of *miR-132* than those from the non-smoker RA patients (Fig. 3*B*). Together, these results demonstrate that AhR-induced *miR-132* in the EVs is closely associated with the inflammatory arthritis in mice and humans.

EVs from Th17 cells induces osteoclastogenesis

The possibility that Th17-derived EVs could contribute to the inflammatory process in arthritis by acting on other immune cells was then explored. Mouse bone marrow-derived DCs were cultured with LPS with or without EVs from Th17. The EVs had no effect on the DCs number or the cytokines (TNF, IL-6, IL-23) produced (*SI Appendix* Fig. S5*A*). Bone marrow-derived macrophages were also cultured under M0 (medium alone), M1 (LPS) or M2 (IL-4) conditions with or without Th17 EVs. The EVs again had no effect on the polarization of macrophages (*SI Appendix* Fig. S5*B*).

Next, we tested the effect of Th17 EVs on osteoclastogenesis. Murine bone marrow derived pre-osteoclasts (pre-OC) were cultured with RANKL/M-CSF in the presence or absence of Th17-derived EVs and the resulting number of $TRAP^+$ multi-nucleated cells determined. The number of osteoclasts (OC) was significantly increased by the presence of EVs from Th17 cells. This number was further elevated by the EVs from Th17 cells previously cultured with FICZ or CSEM. However, these increases were blocked by the presence of GW4869 (Fig. 3*C*).

To confirm the role of *miR-132* in osteoclastogenesis, murine bone marrow pre-OC were differentiated to OC in the presence of RANKL and M-CSF and the level of *miR-132* expression was followed over a 72 h period. Some of the OC were transfected with anti-miR-132 or its scrambled control. The expression of *miR-132* in the OC increased steadily from 48 h of culture. This expression was completely blocked by the transfection of anti-miR-132 (Fig. 3*D*). We then

differentiated pre-OC with RANKL/M-CSF in the presence or absence of EV from Th17 cells, and transfected the OC with anti-miR-132 or the scrambled control. The anti-miR-132 effectively blocked the differentiation of OC by RANKL/M-CSF alone or in combination with Th17 EVs (Fig. 3*E*). These results therefore demonstrate that Th17 cells increase osteoclastogenesis by *miR-132* delivered to the pre-OC via EVs.

miR-132 **inhibits Cox2 induction during OC differentiation**

We then explored the mechanism by which *miR-132* induces osteoclastogenesis. A recent report suggested that *miR-132* could down regulate the expression of *PTGS2* (prostaglandin-endoperoxide synthase 2) gene during human macrophage-OC differentiation (28). *PTGS2* encodes the enzyme cyclooxygenase 2 (COX-2), which catalyzes critical steps in the synthesis of prostaglandins (PGs) from arachidonic acid. PGE2, PGD2 and PGF2 are reported to have inhibitory effects on OC function (29-33). We therefore investigated the role of *Ptgs2* and COX-2 in the induction of osteoclastogenesis by EVs from Th17 cells. Murine pre-OC was cultured with RANKL/M-CSF in the presence of anti-miR-132 or scrambled control. The expression of *Ptsg2* gene was progressively reduced during OC differentiation in a time-dependent manner; and this was reversed by the presence of anti-miR-132 (Fig. 3*F*). This result was confirmed in Western-blot analysis for the level of COX-2 in the differentiated OC. COX-2 protein level was significantly elevated in the OC by the transfection of anti-miR-132 (Fig. 3*G*). We then tested the effect of celecoxib (a well-defined COX-2 inhibitor) on osteoclastogenesis. Pre-OCs were cultured with RANKL/M-CSF in the presence of celecoxib, EVs or anti-miR-132. The number of OC was significantly increased by the blocking of COX-2 with celecoxib; and this increase was further elevated by the presence of EVs of Th17 previously cultured with CSEM (Fig. 3*H*). Strikingly, the increase in the number of OC was inhibited by the presence of anti-miR-132 (Fig. 3*H*). These results show that the *Ptsg2*-Cox2 pathway plays an important role in the *miR-132*-induced OC differentiation mediated by Th17 cell EVs activated by CS.

Anti-miR-132 blocks arthritis and osteoclastogenesis *in vivo*

To determine the role of *miR-132* in osteoclastogenesis *in vivo*, C57BL/6 mice were primed and boosted with mBSA (AIA model) and injected intra-articularly with anti-miR-132 or its scrambled control. Anti-miR-132 injection completely inhibited the expression of *miR-132* in the synovial membrane of the AIA mice (Fig. 4*A*), demonstrating the efficiency of the *in vivo* anti-miR-132 treatment. The inflammatory arthritis was markedly attenuated by the injection of anti-miR-132 as evidenced by the reduction in the joint swelling (Fig. 4*B***)** and histopathological scores of the joints (Fig. 4*C*). In further experiments, AIA mice were exposed to CS and injected with anti-miR-132 or the scrambled control. Histological analysis of the femur-tibial joints revealed marked increase of $TRAP^+$ periarticular cells in mice exposed to CS. This increase was completely abolished by the injection of anti-miR-132 (Fig. 4*D*). These results demonstrate that the exacerbated arthritic inflammation and osteoclastogenesis induced by CS is dependent on *miR-132*.

Discussion

CS is an important environmental factor influencing a range of diseases (34). In this report, we revealed a hitherto unrecognized mechanism by which CS may exacerbate RA (Fig. 4*E*). CS acts as an important agonist for AhR on Th17 cells to induce the expression of *miR-132*. The *miR-132* thus induced is packaged in EVs secreted by the activated Th17 cells. The *miR-132* in EVs then activates osteoclastogenesis by suppressing the transcription of *Ptsg2* and the expression of COX-2 that would otherwise catalyze arachidonic acid to PGs, which have been documented to inhibit osteoclastogenesis (29-33). The result would be the promotion of joint destruction, an event with irreversible consequences for RA patients (35).

Nakahama et al (36) reported that miRNA-132/212 cluster was up-regulated by AHR activation under Th17-inducing condition and that deficiency of this cluster prevented the enhancement of Th17 differentiation by AHR activation. Surprisingly, we could not observe an intrinsic effect of *miR-132* in Th17 cells differentiation or activation. The apparent discrepancy between our findings may

be that miRNAs other than miR132 in the miRNA-132/212 cluster are important in the Th17 differentiation. Instead we found that *miR-132* induced was packaged into Th17-derived EVs. T cells are known to release EVs upon activation, however the importance of vesicular miRNAs in modulate the immune response by these cells is still little explored (37-39). Here we demonstrate that EV containing miR-132 strongly affects the differentiation of osteoclasts *in vitro*. The mechanism by which RNA molecules is sorted into EVs is not completely understood, but it is recognized that important molecules from microRNA silencing complex are present in EVs and contribute to miRNAs function (40, 41). Here, we detected the presence of Ago2 in the Th17 EVs, supporting the functionality of *miR-132*. However, it should be noted that although we have demonstrated that *miRNA-132* in EVs could induce osteoclastogenesis *in vitro*, further study is needed to show directly they affect inflammatory arthritis *in vivo*.

The enzyme COX2 catalyze critical steps in the synthesis of pro-inflammatory prostaglandins (PGs) from arachidonic acid, which plays important roles in bone homeostasis and in pathophysiology of bone disease (42). The PGs effects on osteoclasts function are complex and somewhat contradictory, depending on the PG subtype investigated. Exogenous PGE2, for example, can stimulate osteoclasts formation and bone resorption (43, 44). In contrast, PGE2 exhibit an inhibitory effect on human osteoclasts cells or osteoclasts derived from spleen cultures (29-31). Exogenous PGD2 and PGF2α also have been shown to inhibit osteoclasts function (32, 33). However, endogenous production of eicosanoids by osteoclasts on bone metabolism was unexplored. Here, we demonstrate that Celecoxib, a specific COX2 inhibitor, enhances osteoclast formation. Consistent with our results, it have been demonstrated that osteoclasts express cytosolic phospholipase A2 (cPLA2), responsible for the liberation of arachidonic acid from cellular membrane and subsequent eicosanoid biosynthesis. Pharmacological inhibition of cPLA2 increased osteoclastogenesis (45), suggesting that its activity and subsequent metabolites would exert a negative control of osteoclasts function. The precise mechanism of COX2 modulation of endogenous PGs in osteoclastogenesis and its functional role *in vivo* remains to be explored.

Our finding in the murine arthritic models appears to be applicable to clinical RA. $CD4^+$ T cells from the peripheral blood of the RA patients expressed significantly higher levels of *miR-132* compared to that of the cells from the healthy controls. Furthermore, $CD4^+$ T cells from the smoker RA patients expressed significantly higher level of *miR-132* than that of the cells from the non-smokers. Moreover, the EVs from smoker RA patients expressed significantly higher levels of *miR-132* than those from the non-smoker RA patients. Together, these results demonstrate that AhR-induced *miR-132* in the EVs is closely associated with clinical RA. It would be important to further explore *miR-132* as a therapeutic target to alleviate inflammation and bone damage in RA.

Materials and Methods

Mice, induction of arthritis. Male C57BL/6, DBA/1J and *Ahr*$^{-/-}$mice were bred in specific pathogen-free animal facility at the School of Medicine of Ribeirão Preto, University of São Paulo, Brazil. All experiments were performed in accordance to the guidelines outlined by Standing Committee on Animals at Ribeirão Preto Medical School, University of Sao Paulo (n^o 048/2012). *Ahr*$^{-/-}$ mice on the C57BL/6 background were provided by Dr Frank Gonzalez (National Cancer Institute, National Institute of Health, Bethesda, USA). For induction of antigen-induced arthritis (AIA) C57BL/6 mice were injected subcutaneously with methylated BSA in CFA and boosted with the same preparation in IFA. For collagen-induced arthritis (CIA), DBA/1J mice were injected intradermally with bovine type II collagen in CFA. Detailed information describing protocols for T cell differentiation, osteoclast cultures, microarrays, flow cytometry, extracellular vesicles purification and analysis, anti-MiR transfections, cigarette smoke exposure is provided in *SI Appendix*.

Patients and Healthy donors. Peripheral blood samples from 37 RA patients and 34 healthy individuals were obtained from CD4+ T cells analysis. All patients fulfilled the 2010 American College of Rheumatology and European League against Rheumatism criteria for RA classification (46), and did not receive any treatment. Disease activity was measured by DAS28 (Disease Activity Score, including a 28-joint count), and RA patients were stratified according to smoking in smokers

and non-smokers. Synovial liquid from 22 RA patients were also collected for isolation of extracellular vesicles. The clinical features of the subjects are detailed *Table S2*. All donors provided informed consent to participate in the study, approved by the Research Ethics Committee of HCFMRP – University of São Paulo (Protocol 5776/2015). Subjects presenting other autoimmune or rheumatic diseases and infectious disorders or were serologic positive for Chagas disease, hepatitis B and C, or HIV were excluded. All laboratory analyses of the samples were performed blind to the donor status. Further information is provided in *SI Appendix*.

Acknowledgements

We thank Sergio L. C. Almeida, Patricia Rolim and members of the Rheumatoid Arthritis team for their advice and clinical assistance; Dr Fausto Almeida research group for their support at Nanosight analysis. We also thank Ieda R.S. Schivo, Sergio R. Rosa, Ana Katia dos Santos, Denise Ferraz, and Tadeu F. Vieira (in memory) for technical assistance. This work was supported by grants from the São Paulo Research Foundation (FAPESP, 2012/02438-0 and 2013/08216-2 Center for Research in Inflammatory Disease) and from the University of São Paulo (NAP-DIN, 11.1.21625.01.0).

Competing Interests statement

The authors declare no competing interests.

References

1. G. S. Firestein, Evolving concepts of rheumatoid arthritis. *Nature* **423**, 356-361 (2003).
2. I. B. McInnes, G. Schett, The pathogenesis of rheumatoid arthritis. *N Engl J Med* **365**, 2205-2219 (2011).
3. J. S. Smolen *et al.*, Rheumatoid arthritis. *Nat Rev Dis Primers* **4**, 18001 (2018).
4. H. Källberg *et al.*, Smoking is a major preventable risk factor for rheumatoid arthritis: estimations of risks after various exposures to cigarette smoke. *Ann Rheum Dis* **70**, 508-511 (2011).
5. J. Sokolove *et al.*, Increased inflammation and disease activity among current cigarette smokers with rheumatoid arthritis: a cross-sectional analysis of US veterans. *Rheumatology (Oxford)* **55**, 1969-1977 (2016).

6. Y. Ishikawa, C. Terao, The Impact of Cigarette Smoking on Risk of Rheumatoid Arthritis: A Narrative Review. *Cells* **9** (2020).
7. M. S. Denison, S. R. Nagy, Activation of the aryl hydrocarbon receptor by structurally diverse exogenous and endogenous chemicals. *Annu Rev Pharmacol Toxicol* **43**, 309-334 (2003).
8. L. Stejskalova, Z. Dvorak, P. Pavek, Endogenous and exogenous ligands of aryl hydrocarbon receptor: current state of art. *Curr Drug Metab* **12**, 198-212 (2011).
9. J. Talbot *et al.*, Smoking-induced aggravation of experimental arthritis is dependent of aryl hydrocarbon receptor activation in Th17 cells. *Arthritis Res Ther* **20**, 119 (2018).
10. B. Stockinger, P. Di Meglio, M. Gialitakis, J. H. Duarte, The aryl hydrocarbon receptor: multitasking in the immune system. *Annu Rev Immunol* **32**, 403-432 (2014).
11. M. Veldhoen *et al.*, The aryl hydrocarbon receptor links TH17-cell-mediated autoimmunity to environmental toxins. *Nature* **453**, 106-109 (2008).
12. Y. Z. Gu, J. B. Hogenesch, C. A. Bradfield, The PAS superfamily: sensors of environmental and developmental signals. *Annu Rev Pharmacol Toxicol* **40**, 519-561 (2000).
13. M. Adachi *et al.*, Cigarette smoke condensate extracts induce IL-1-beta production from rheumatoid arthritis patient-derived synoviocytes, but not osteoarthritis patient-derived synoviocytes, through aryl hydrocarbon receptor-dependent NF-kappa-B activation and novel NF-kappa-B sites. *J Interferon Cytokine Res* **33**, 297-307 (2013).
14. S. Kobayashi *et al.*, A role for the aryl hydrocarbon receptor and the dioxin TCDD in rheumatoid arthritis. *Rheumatology (Oxford)* **47**, 1317-1322 (2008).
15. F. J. Quintana *et al.*, Control of T(reg) and T(H)17 cell differentiation by the aryl hydrocarbon receptor. *Nature* **453**, 65-71 (2008).
16. A. Kimura, T. Naka, K. Nohara, Y. Fujii-Kuriyama, T. Kishimoto, Aryl hydrocarbon receptor regulates Stat1 activation and participates in the development of Th17 cells. *Proc Natl Acad Sci U S A* **105**, 9721-9726 (2008).
17. T. Nakahama *et al.*, Aryl hydrocarbon receptor deficiency in T cells suppresses the development of collagen-induced arthritis. *Proc Natl Acad Sci U S A* **108**, 14222-14227 (2011).
18. I. I. Ivanov *et al.*, The orphan nuclear receptor RORgammat directs the differentiation program of proinflammatory IL-17+ T helper cells. *Cell* **126**, 1121-1133 (2006).
19. K. Sato *et al.*, Th17 functions as an osteoclastogenic helper T cell subset that links T cell activation and bone destruction. *J Exp Med* **203**, 2673-2682 (2006).
20. N. Komatsu *et al.*, Pathogenic conversion of Foxp3+ T cells into TH17 cells in autoimmune arthritis. *Nat Med* **20**, 62-68 (2014).
21. V. Ambros, The functions of animal microRNAs. *Nature* **431**, 350-355 (2004).
22. B. M. Engels, G. Hutvagner, Principles and effects of microRNA-mediated post-transcriptional gene regulation. *Oncogene* **25**, 6163-6169 (2006).

23. K. M. Pauley *et al.*, Upregulated miR-146a expression in peripheral blood mononuclear cells from rheumatoid arthritis patients. *Arthritis Res Ther* **10**, R101 (2008).
24. K. Murata *et al.*, Plasma and synovial fluid microRNAs as potential biomarkers of rheumatoid arthritis and osteoarthritis. *Arthritis Res Ther* **12**, R86 (2010).
25. R. M. O'Connell, D. S. Rao, A. A. Chaudhuri, D. Baltimore, Physiological and pathological roles for microRNAs in the immune system. *Nat Rev Immunol* **10**, 111-122 (2010).
26. R. M. Johnstone, Exosomes biological significance: A concise review. *Blood Cells Mol Dis* **36**, 315-321 (2006).
27. H. Valadi *et al.*, Exosome-mediated transfer of mRNAs and microRNAs is a novel mechanism of genetic exchange between cells. *Nat Cell Biol* **9**, 654-659 (2007).
28. L. de la Rica *et al.*, NF-κB-direct activation of microRNAs with repressive effects on monocyte-specific genes is critical for osteoclast differentiation. *Genome Biol* **16**, 2 (2015).
29. K. Ono *et al.*, Biphasic effect of prostaglandin E2 on osteoclast formation in spleen cell cultures: role of the EP2 receptor. *J Bone Miner Res* **20**, 23-29 (2005).
30. T. Shibata-Nozaki *et al.*, Endogenous prostaglandin E2 inhibits aberrant overgrowth of rheumatoid synovial tissue and the development of osteoclast activity through EP4 receptor. *Arthritis Rheum* **63**, 2595-2605 (2011).
31. I. Take *et al.*, Prostaglandin E2 strongly inhibits human osteoclast formation. *Endocrinology* **146**, 5204-5214 (2005).
32. M. Durand, M. A. Gallant, A. J. de Brum-Fernandes, Prostaglandin D2 receptors control osteoclastogenesis and the activity of human osteoclasts. *J Bone Miner Res* **23**, 1097-1105 (2008).
33. X. Xu *et al.*, The prevention of latanoprost on osteoclastgenesis in vitro and lipopolysaccharide-induced murine calvaria osteolysis in vivo. *J Cell Biochem* **119**, 4680-4691 (2018).
34. C. Perricone *et al.*, Smoke and autoimmunity: The fire behind the disease. *Autoimmun Rev* **15**, 354-374 (2016).
35. G. Schett, E. Gravallese, Bone erosion in rheumatoid arthritis: mechanisms, diagnosis and treatment. *Nat Rev Rheumatol* **8**, 656-664 (2012).
36. T. Nakahama *et al.*, Aryl hydrocarbon receptor-mediated induction of the microRNA-132/212 cluster promotes interleukin-17-producing T-helper cell differentiation. *Proc Natl Acad Sci U S A* **110**, 11964-11969 (2013).
37. M. Mittelbrunn *et al.*, Unidirectional transfer of microRNA-loaded exosomes from T cells to antigen-presenting cells. *Nat Commun* **2**, 282 (2011).
38. I. S. Okoye *et al.*, MicroRNA-Containing T-Regulatory-Cell-Derived Exosomes Suppress Pathogenic T Helper 1 Cells. *Immunity* **41**, 503 (2014).
39. L. N. Ventimiglia, M. A. Alonso, Biogenesis and Function of T Cell-Derived Exosomes. *Front Cell Dev Biol* **4**, 84 (2016).

40. J. Guduric-Fuchs *et al.*, Selective extracellular vesicle-mediated export of an overlapping set of microRNAs from multiple cell types. *BMC Genomics* **13**, 357 (2012).
41. S. A. Melo *et al.*, Cancer exosomes perform cell-independent microRNA biogenesis and promote tumorigenesis. *Cancer Cell* **26**, 707-721 (2014).
42. K. A. Blackwell, L. G. Raisz, C. C. Pilbeam, Prostaglandins in bone: bad cop, good cop? *Trends Endocrinol Metab* **21**, 294-301 (2010).
43. H. Kaji *et al.*, Prostaglandin E2 stimulates osteoclast-like cell formation and bone-resorbing activity via osteoblasts: role of cAMP-dependent protein kinase. *J Bone Miner Res* **11**, 62-71 (1996).
44. X. Y. Tian *et al.*, Continuous infusion of PGE2 is catabolic with a negative bone balance on both cancellous and cortical bone in rats. *J Musculoskelet Neuronal Interact* **7**, 372-381 (2007).
45. H. Allard-Chamard, P. Dufort, S. Haroun, A. J. de Brum-Fernandes, Cytosolic phospholipase A2 and eicosanoids modulate life, death and function of human osteoclasts in vitro. *Prostaglandins Leukot Essent Fatty Acids* **90**, 117-123 (2014).
46. D. Aletaha *et al.*, 2010 Rheumatoid arthritis classification criteria: an American College of Rheumatology/European League Against Rheumatism collaborative initiative. *Arthritis Rheum* **62**, 2569-2581 (2010).

Fig. 1. AhR activation induces the expression of specific miRNAs in Th17 cells. Naïve T cells ($CD4^+CD44^-CD62L^+$) were activated with plate-bound anti-CD3 and soluble anti-CD28, and polarized to Th17 with a cocktail of TGF-β1, IL-6, and IL-1β for 72 h. (*A*) Heatmap of miRNA significantly expressed (fold-change $\geq$ 2.0 and FDR $<$ 5%) in IL-17-producing $CD4^+$ T cells cultured for a further 24 h with the cytokine cocktail plus IL-23 with or without FICZ. $CD4^+$ T cells cultured in the presence of IL-2 were used as control (Th0). (*B*) miRNAs homologous sequence between mice and human obtained from miRBase. qPCR analysis of (*C*) *miR-132, miR-346*, and (*D*) *Cyp1a1* in Th17 cells. Results were calculated by the comparative threshold cycle method. (*E*) Representative dot plot of $CD4^+$ IL-$17A^+$ T cells frequency assessed by flow cytometry, and frequency of $CD4^+$ IL-$17A^+$ T cells. (*F*) ELISA of IL-22 in the supernatants of Th17 cells differentiation as in (*E*). Data are mean $\pm$ SEM, representative of three independent experiments. Statistical analysis was performed by unpaired, two-tailed Student's *t*-test (n $\geq$ 3/group).

Fig. 2. AhR activation-induced miRNAs are associated with arthritis. qPCR *for miR-132*, and *miR-346* expression in $CD4^+$ $IL\text{-}17^+$ T cells isolated from draining lymph nodes of (*A*) WT C57BL/6 or AhR-deficient mice in the AIA model, (*B*) DBA-1/J mice in the CIA model. Mice were treated with FICZ or vehicle (DMSO). (*C*) *MiR-132*, *miR-346* and *Cyp1a1* expression in AIA mice exposed or not to cigarette smoke during immunization. (*D*) MiRNA expression in CIA mice exposed or not to cigarette smoke as in (*C*). Data are representative of three independent experiments, and $IL\text{-}17^+$ cells were pooled from 3 mice (mean ± SEM). Results were calculated by the comparative threshold cycle method. Statistical analysis was performed by one-way ANOVA followed by Bonferroni test, or unpaired, two-tailed Student's *t*-test ($n \geq 3$/group). (*E*, *F*) $CD4^+$ T cells were isolated from the peripheral blood of RA patients (n=37) or healthy controls (n=34). Total RNA was extracted for qPCR analysis. (*E*) Expression of *miR-132* and *miR-346* in the T cells from controls and RA patients. (*F*) *MiR-132, miR-346*, and *CYP1A1* expression in the T cells from non-smokers (n=18) and smokers (n=19) RA patients. Results were calculated by the comparative threshold cycle method and are presented relative to that of *RNU48* (internal control miRNA), or *GAPDH* (internal control). NS = not significant. Statistical analysis was performed by nonparametric Mann-Whitney test.

Fig. 3. AhR-induced *miR-132* is released by Th17 in extracellular vesicles and promotes osteoclastogenesis. Naïve T cells ($CD4^+CD44^-CD62L^+$) were polarized to Th17 for 72 h (as in Fig. 1*A*) with or without FICZ, CSEM (CS-enriched medium) or GW4869 (a vesicle blocking agent). Culture supernatants were collected and extracellular vesicles (EVs) isolated by ultracentrifugation. (*A*) Equal numbers of purified EVs were collected for qPCR analysis for *miRNA-132*. Statistical analysis was performed by one-way ANOVA followed by Bonferroni test. Data are representative of three independent experiments. ND, not detectable. (*B*) *miRNA-132* expression in EVs of the synovial fluids from non-smoker (n=11) and smoker (n=11) RA patients. Results were calculated by the comparative threshold cycle method and are presented relative to that of *miR-361* (internal control miRNA). Statistical analysis was performed by nonparametric Mann-Whitney test. (*C*)

Osteoclasts (OCs) were differentiated with RANKL and M-CSF in the presence of EVs from Th17 supernatants previously treated with vehicle, FICZ, CSEM or GW4869. Images and number of $TRAP^+$ multinuclear OCs (scale bar 75 μm) are shown. (*D*) *MiR-132* expression during OC differentiation. (*E*) OCs were differentiated (as in *C*) in the presence of EVs from Th17, and transfected with anti-miR-132 or scrambled control. Images and number of $TRAP^+$ multinuclear OC (scale bar 75 μm) are shown. (*F*) Heatmap of *Ptgs2* expression in OCs differentiated in the presence of anti-miR-132 or scrambled control. (*G*) OCs collected after 72 h were analyzed by western blot for the presence of COX-2. Statistical analysis was performed by unpaired, two-tailed Student's *t*-test. Data (mean ± SEM) are from two independent experiments. (*H*) OCs were differentiated in the presence of RANKL and M-CSF for 48 h and then re-stimulated for 24 h with M-CSF and RANKL in the presence or absence of EVs isolated from Th17 pre-treated with CSEM or a COX-2 inhibitor, celecoxib. Some cells were also transfected with anti-miR-132. Representative images (scale bar 75 μm) and number of multinuclear $TRAP^+$ OCs are shown. Statistical analysis was performed by one-way ANOVA followed by Bonferroni test, or unpaired, two-tailed Student's *t*-test ($n \geq 3$/group). Data (mean ± SEM) are representative of two independent experiments.

Fig. 4. Anti-miR-132 blocks arthritis and osteoclastogenesis *in vivo*. (*A*) *MiR-132* expression in the total synovial membrane of AIA mice injected intra-articularly with PBS (sham), miRCURY LNA anti-miR-132 or scrambled control. ND, not detectable. Inflammatory arthritis of AIA mice (treated as in *A*) was measured as Δ joint diameter (*B*), and histopathological score (*C*). (*D*) AIA mice were exposed to CS and injected intra-articularly with anti-miR-132 or scrambled control. Images and number of periarticular $TRAP^+$ cells in the femur-tibial joint (scale bar 200 μm) are shown. Statistical analysis was performed by one-way ANOVA followed by Bonferroni test, or unpaired, two-tailed Student's *t*-test. Data are mean ± SEM, representative of two independent experiments ($n \geq 3$/group). (*E*) Schematic representation of the regulation and function of *miR-132* on osteoclastogenesis in RA.

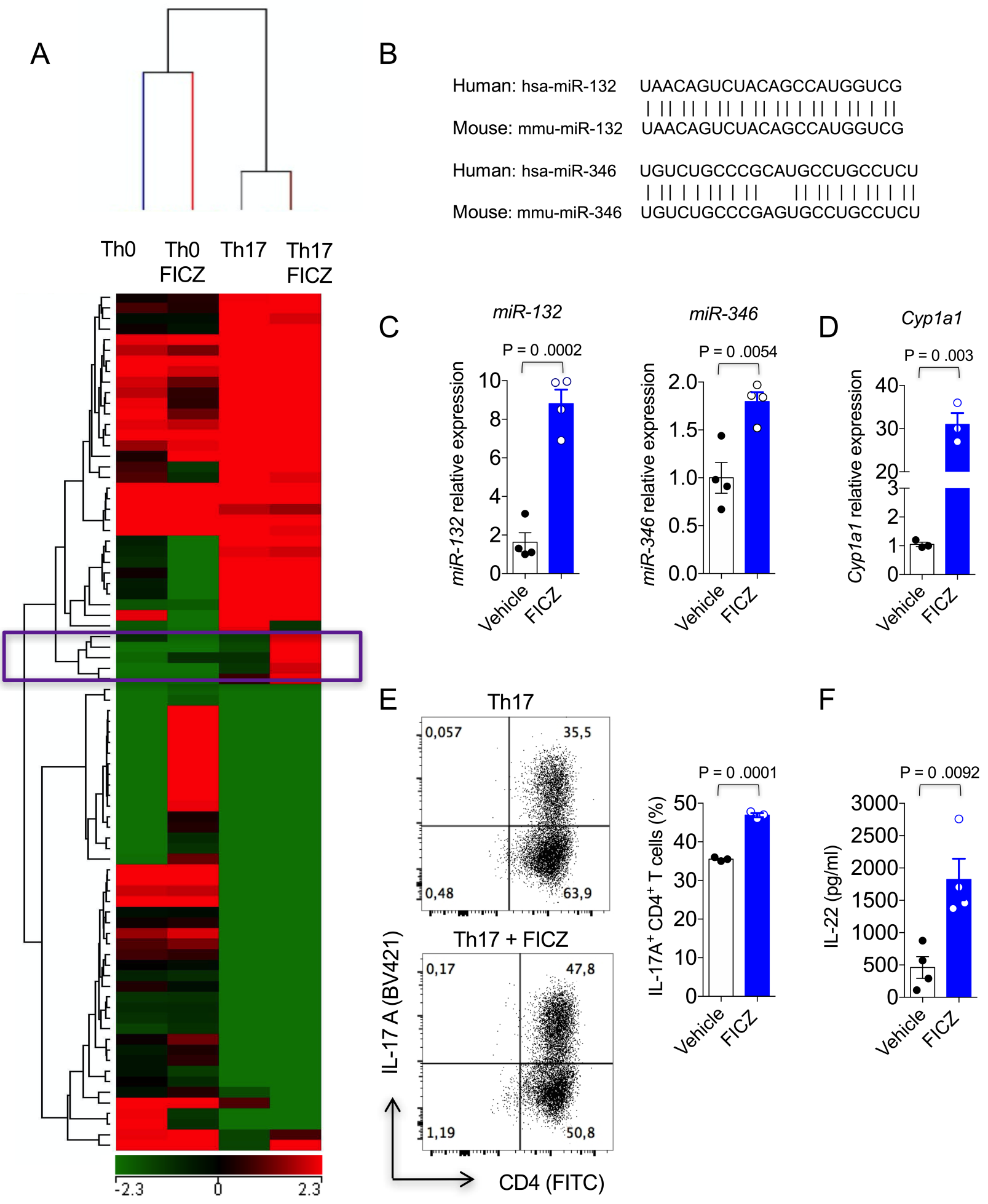
A
Th0
Th0 FICZ
Th17
Th17 FICZ
-2.3
0
2.3
B
Human: hsa-miR-132 UAACAGUCUACAGCCAUGGUCG
Mouse: mmu-miR-132 UAACAGUCUACAGCCAUGGUCG
Human: hsa-miR-346 UGUCUGCCCGCAUGCCUGCCUCU
Mouse: mmu-miR-346 UGUCUGCCCGAGUGCCUGCCUCU
C
miR-132
P = 0 .0002
miR-132 relative expression
Vehicle
FICZ
miR-346
P = 0 .0054
miR-346 relative expression
D
Cyp1a1
P = 0 .003
Cyp1a1 relative expression
E
Th17
0,057
35,5
0,48
63,9
Th17 + FICZ
0,17
47,8
1,19
50,8
IL-17 A (BV421)
CD4 (FITC)
P = 0 .0001
IL-17A+ CD4+ T cells (%)
F
P = 0 .0092
IL-22 (pg/ml)

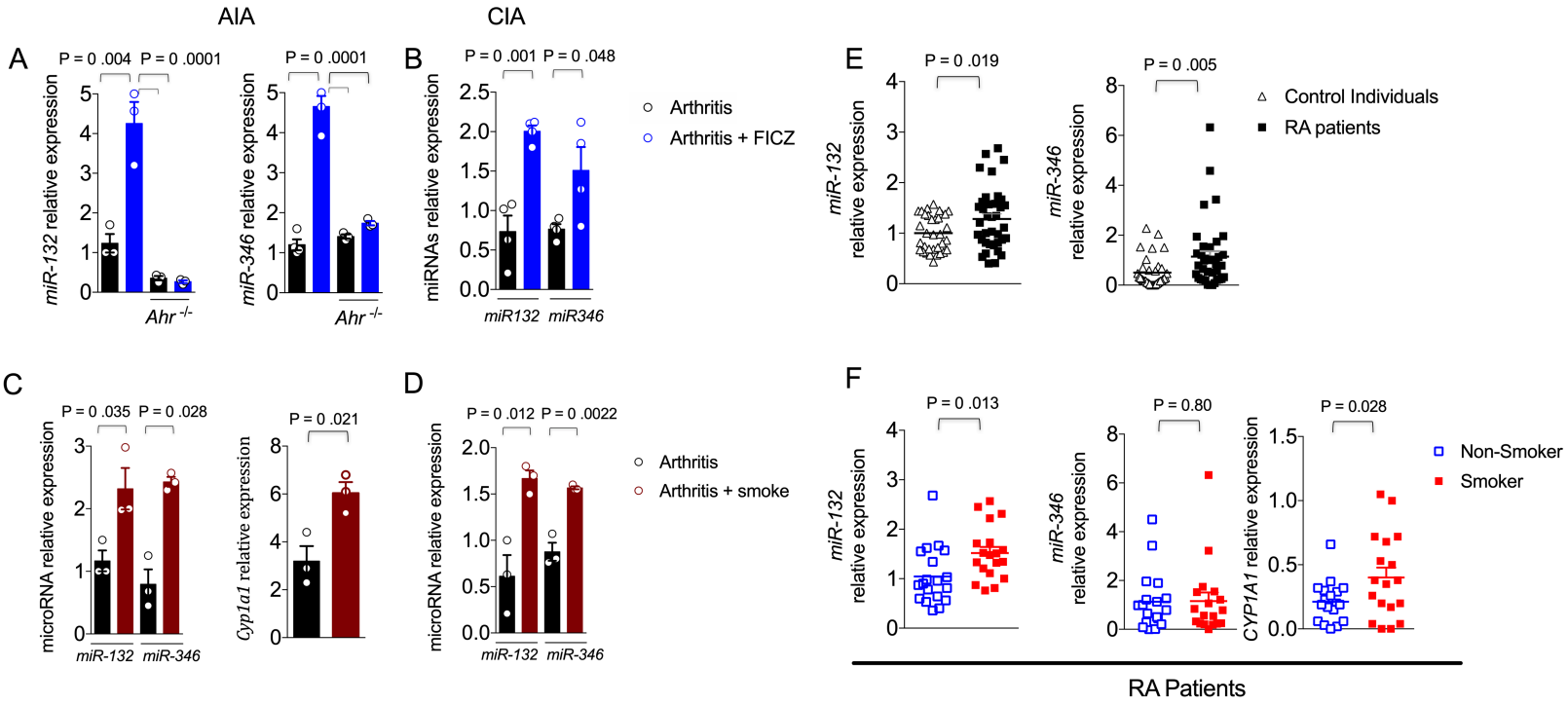
AIA
CIA
A
P = 0 .004
P = 0 .0001
miR-132 relative expression
Ahr -/-
P = 0 .0001
miR-346 relative expression
Ahr -/-
B
P = 0 .001
P = 0 .048
miRNAs relative expression
miR132
miR346
Arthritis
Arthritis + FICZ
C
P = 0 .035
P = 0 .028
microRNA relative expression
miR-132
miR-346
P = 0 .021
Cyp1a1 relative expression
D
P = 0 .012
P = 0 .0022
microRNA relative expression
miR-132
miR-346
Arthritis
Arthritis + smoke
E
P = 0 .019
miR-132 relative expression
P = 0 .005
miR-346 relative expression
Control Individuals
RA patients
F
P = 0 .013
miR-132 relative expression
P = 0.80
miR-346 relative expression
P = 0.028
CYP1A1 relative expression
Non-Smoker
Smoker
RA Patients

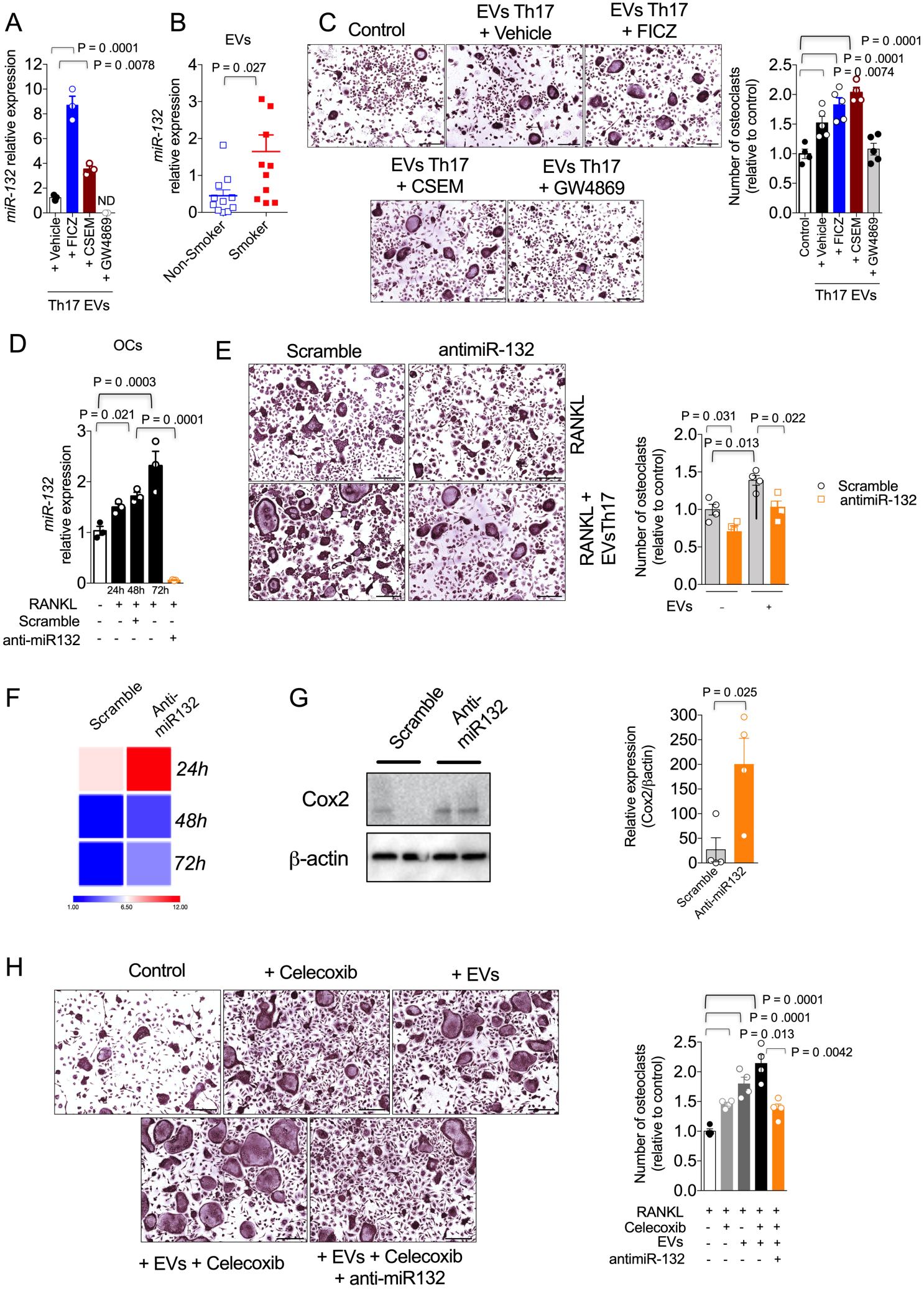
A
P = 0 .0001
P = 0 .0078
miR-132 relative expression
ND
+ Vehicle
+ FICZ
+ CSEM
+ GW4869
Th17 EVs
B
EVs
P = 0 .027
miR-132 relative expression
Non-Smoker
Smoker
C
Control
EVs Th17 + Vehicle
EVs Th17 + FICZ
EVs Th17 + CSEM
EVs Th17 + GW4869
P = 0 .0001
P = 0 .0001
P = 0 .0074
Number of osteoclasts (relative to control)
Control
+ Vehicle
+ FICZ
+ CSEM
+ GW4869
Th17 EVs
D
OCs
P = 0 .0003
P = 0 .021
P = 0 .0001
miR-132 relative expression
24h 48h 72h
RANKL
Scramble
anti-miR132
E
Scramble
antimiR-132
RANKL
RANKL + EVsTh17
P = 0 .031
P = 0 .022
P = 0 .013
Number of osteoclasts (relative to control)
Scramble
antimiR-132
EVs
F
Scramble
Anti-miR132
24h
48h
72h
1.00
6.50
12.00
G
Scramble
Anti-miR132
Cox2
β-actin
P = 0 .025
Relative expression (Cox2/βactin)
Scramble
Anti-miR132
H
Control
+ Celecoxib
+ EVs
+ EVs + Celecoxib
+ EVs + Celecoxib + anti-miR132
P = 0 .0001
P = 0 .0001
P = 0 .013
P = 0 .0042
Number of osteoclasts (relative to control)
RANKL
Celecoxib
EVs
antimiR-132

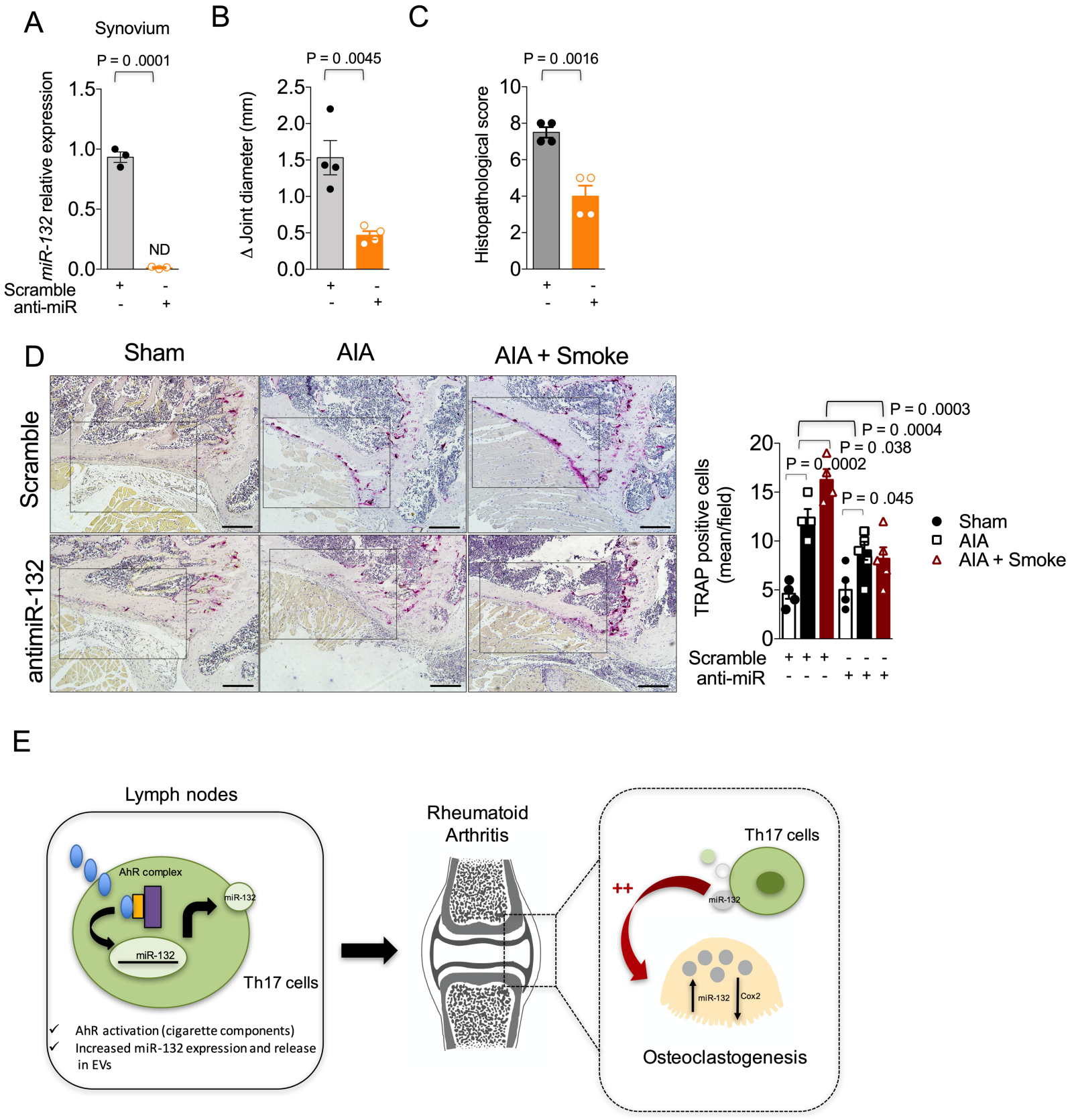
A
Synovium
P = 0 .0001
miR-132 relative expression
1.5
1.0
0.5
0.0
ND
Scramble
anti-miR
+
-
-
+
B
P = 0 .0045
Δ Joint diameter (mm)
2.5
2.0
1.5
1.0
0.5
0.0
C
P = 0 .0016
Histopathological score
10
8
6
4
2
0
D
Sham
AIA
AIA + Smoke
Scramble
antimiR-132
P = 0 .0003
P = 0 .0004
P = 0 .038
P = 0 .0002
P = 0 .045
TRAP positive cells (mean/field)
20
15
10
5
0
Sham
AIA
AIA + Smoke
E
Lymph nodes
AhR complex
miR-132
miR-132
Th17 cells
AhR activation (cigarette components)
Increased miR-132 expression and release in EVs
Rheumatoid Arthritis
Th17 cells
++
miR-132
miR-132
Cox2
Osteoclastogenesis